Green Chemistry

Accepted Manuscript

ROYAL SOCIETY OF CHEMISTRY

www.rsc.org/greenchem

Journal Name

Dynamic Article Links ▶

ARTICLE TYPE

Asymmetric hydrogenation in nanoreactors with encapsulated Rh-MonoPhos catalyst

Mingmei Zhong [abc], **Xiaoming Zhang** [abc], **Yaopeng Zhao** [a], **Can Li*** [a], **Qihua Yang*** [a]

The asymmetric multicomponent catalyst, Rh-MonoPhos, was successfully encapsulated in the nanocages of mesoporous silicas with cage-like structure (FDU-12 and C-FDU-12). The resulting solid catalyst exhibits excellent activity (TOF 2052 h^{-1}) and enantioselectivity (93% ee) in the asymmetric hydrogenation of olefin derivatives. The solid catalyst with Rh(MonoPhos)$_2$ in nanocages affords much

10 higher activity than that with Rh(MonoPhos)$_1$ or Rh(MonoPhos)$_3$ in nanocages. Combined with the ESI-MS results, it could be supposed that RhL$_2$(nbd) may be active species or the precursors for active species. Moreover, the solid catalyst with C-FDU-12 (inner surface modified by a thin carbon layer) as host material shows much higher activity and enantioselectivity than that with pure silica FDU-12 as host material in the asymmetric hydrogenation of different kinds of olefin derivatives, indicating that the

15 microenvironment modification is one of the key factors for improving the catalytic performance of the solid catalyst. The solid catalysts possess high stability and could be reused for at least 7 times.

Introduction

The production of chiral compounds via green and atomic efficient route is a long term pursue in industry. Up to date, most

20 chiral compounds are produced via two methods, stoichiometric organic transformation and chiral separation, which are often neither "green" nor atomic efficient. Thanks to recent progress in organometallic chemistry, various kinds of chiral metal complexes have been developed for asymmetric catalysis.[1]

25 Though some chiral compounds could be efficiently produced via asymmetric catalytic approach, the product purification and recycling of expensive chiral metal complexes still remain a problem because chiral metal complexes are usually dissolved in the same phase with reactants and products. To solve this

30 problem, the chiral metal complexes have usually been immobilized onto solid supports (SiO$_2$, clay, Al$_2$O$_3$, carbon ect.)[2] via adsorption, electrostatic interaction,[3] covalent grafting[4] and so on. The altered microenvironment of chiral metal complexes and the diffusion barriers of the solid support often cause decrease in

35 activity and enantioselectivity after immobilization[5]. Encouragingly, the positive effect of solid supports on the performance of immobilized chiral catalysts has been reported in some cases, such as the pore confinement effect for enhancing the enantioselectivity,[6] the enrichment effect for increasing both the

40 catalytic activity and the enantioselectivity,[7] and so on. Thus, carefully choosing the immobilization method and the support material based on the nature of chiral catalysts may help to improve the catalytic performance of the immobilized chiral catalysts.

45 Asymmetric hydrogenation of prochiral olefins, imines, and ketones is an attractive methodology for obtaining optically active molecules which are usually important intermediates for pharmaceuticals and agrochemicals.[8] Among various metal complexes, the monodentate phosphorous ligands based catalysts

50 have gained much research interests owning to their efficiency, easy preparation and stability.[9] However, compared with metal complexes of bidentate ligands with well-defined molecular structure and active sites, the metal complexes formed with monodentate phosphorous ligand often involve the co-existence

55 of a dynamic mixture of different kinds of metal complexes equilibrating with each other in solution. Usually, only one metal complex is the active or the most active catalyst and the reaction conditions, such as ligand-to-metal ratio and solvent, often have great influence on the catalytic performance. As a result, not only

60 the usage efficiency of the catalyst is not high but also the mechanism investigation for elucidating the active species for the catalytic reaction is very difficult.

So far, several strategies have been developed for the immobilization of multicomponent catalysts with monodentate

65 phosphorous ligands.[10] Ding and co-workers demonstrated a successful immobilization of Rh-MonoPhos via a self-supported strategy for enantioselective hydrogenation of α-dehydroamino acid and enamide derivatives.[11] Sheldon and co-workers reported the immobilization of Rh-MonoPhos on the aluminosilicate

70 support by ionic interactions and the resulting heterogeneous catalyst showed excellent enantioselectivity and activity in the asymmetric hydrogenation of methyl-2-acetamidoacrylate.[12] Our group described a facile adsorption strategy for fabricating highly efficient solid catalysts by using the high affinity of silica towards

75 the metal complex and the low solubility of Rh-MonoPhos in hexane.[13] However, the stability and efficiency of the chiral solid catalyst still need to be further improved. Most reported solid

Green Chemistry Accepted Manuscript

catalysts are related with the immobilization of Rh-MonoPhos with ligand-to-metal ratio of 2. Little work investigated the influence of ligand-to-metal ratio on the catalytic performance of solid catalysts, which may help to understand the active species for the reaction.

Our previous study has demonstrated that equilibration between different species for the multicomponent catalysts could be greatly inhibited in a confined nanospace.[14] Inspired by this work, we herein report the encapsulation of the multicomponent metal complex, Rh-MonoPhos, in nanocages of mesoporous silicas with cage-like structure (FDU-12 and C-FDU-12) (scheme 1). The influence of different MonoPhos-to-Rh ratio and microenvironment of nanocages on the catalytic performance of immobilized catalyst were also investigated.
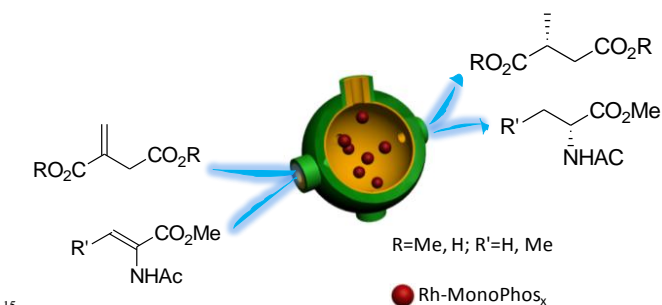
Scheme 1. Schematic illustration for the asymmetric hydrogenation in nanoreactors with encapsulated Rh-MonoPhos.
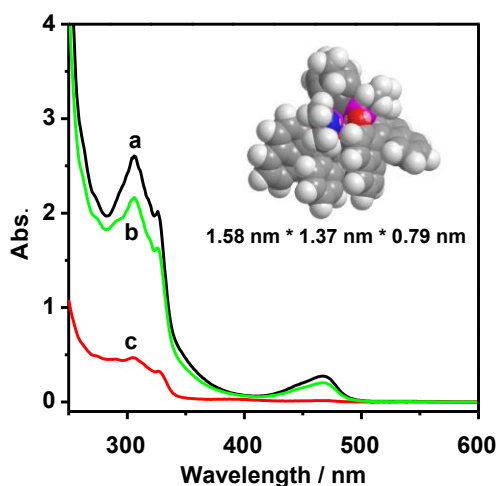
Fig.1 UV-Vis spectra of (a) Rh(MonoPhos)$_2$ in dichloromethane (b) after adsorption with FDU-12-TMOS (FDU-12 silylated with TMOS) or (c) after adsorption with FDU-12.

Results and discussion

Mesoporous silica FDU-12 with cage-like pore structure is used as support for the encapsulation of Rh-MonoPhos complex. TMOS which can hydrolyze and condense easily even in neutral conditions is used as encapsulation reagent. H$_2$O is chosen to promote the silylation process of TMOS. To investigate the influence of microenvironments on the catalytic performance of Rh-MonoPhos, C-FDU-12 with a thin layer of carbon species in the inner surface which is synthesized by carbonization of as-made FDU-12 under inert gas conditions is also chosen as the support.

For simplifying the discussion, Rh-MonoPhos prepared with MonoPhos/Rh ratio of 1, 2 and 3 were denoted as Rh(MonoPhos)$_1$, Rh(MonoPhos)$_2$ and Rh(MonoPhos)$_3$, respectively. The efficiency of TMOS silylation in preventing Rh-MonoPhos complex escaping from the nanoreactor is characterized by adsorption experiment using Rh(MonoPhos)$_2$ (molecular size is about 1.58 nm * 1.37 nm * 0.79 nm) as a probe molecule. UV-Vis spectra of Rh(MonoPhos)$_2$ in dichloromethane before and after adsorption with FDU-12 and FDU-12-TMOS (FDU-12 silylated with TMOS) are shown in Fig. 1. The intensity of the UV-Vis bands decreases sharply comparing with the original solution after adsorption with FDU-12, which means that the pore entrance size of FDU-12 is large enough for Rh(MonoPhos)$_2$ to enter the nanocages. However, after adsorption with FDU-12-TMOS, the intensity of the UV-Vis bands remains almost the same as that of the original Rh(MonoPhos)$_2$ solution, indicating that silylation using TMOS could reduce the pore entrance size smaller than 1.37 nm to prevent the diffusion of Rh(MonoPhos)$_2$ into the nanocages of FDU-12. This means that TMOS silylation could effectively encapsulate Rh(MonoPhos)$_2$ within the nanocages of FDU-12. Rh(MonoPhos)$_n$@FDU-12 and Rh(MonoPhos)$_2$@C-FDU-12 was successfully prepared by encapsulation method with TMOS as silylation reagent. The content of encapsulated Rh(MonoPhos)$_2$ could be tuned from 0.03 to 0.16 mmol/g by changing the amount of Rh(MonoPhos)$_2$ in the adsorption step (Table 1). Notably, 62-85% of Rh(MonoPhos)$_2$ employed in the adsorption step could be successfully encapsulated in the nanocages, showing that this method is very efficient.
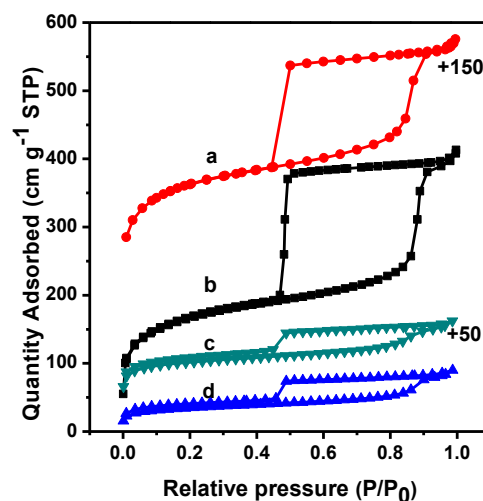
Fig.2 Nitrogen adsorption-desorption isotherms of (a) C-FDU-12, (b) FDU-12, (c) Rh(MonoPhos)$_2$@C-FDU-12 (0.13 mmol Rh /g) and (d) Rh(MonoPhos)$_2$@FDU-12 (0.12 mmol Rh /g).

Table 1. Textural parameters of supports and solid catalysts and the content of Rh(MonoPhos)$_n$ in solid catalysts.

Sample	BET surface area (m^2/g)[a]	Total pore volume (cm^3/g)[b]	Micropore volume (cm^3/g)	Pore size (nm)[c]	Rh content (mmol/g)	Encapsulation efficiency (%)[d]	Molecular number per cage[e]
FDU-12	653	0.61	0.109	14.8	--	--	--
C-FDU-12	746	0.64	0.140	14.3	--	--	--
Rh(MonoPhos)$_2$@FDU-12	360	0.41	0.072	16.4	0.03	62	63
Rh(MonoPhos)$_2$@FDU-12	223	0.24	0.042	16.2	0.07	71	144
Rh(MonoPhos)$_2$@FDU-12	120	0.14	0.022	16.4	0.12	78	237
Rh(MonoPhos)$_2$@FDU-12	45	0.057	0.006	16.3	0.16	78	318
Rh(MonoPhos)$_1$@FDU-12	337	0.38	0.067	15.9	0.12	79	243
Rh(MonoPhos)$_3$@FDU-12	229	0.18	0.058	16.7	0.10	69	212
Rh(MonoPhos)$_2$@C-FDU-12	244	0.20	0.064	14.0	0.13[f]	85	235

[a] BET surface area. [b] Pore volume calculated at relative pressure P/Po of 0.99. [c] BJH method from adsorption branch. [d] Calculated the amount of MonoPhos-Rh encapsulating in solid catalyst / the amount of MonoPhos-Rh in the adsorption step. [e] Calculated according the formula $\mathbf{n} = \frac{N_{Rh(1g)} \times 6.02 \times 10^{23}}{\frac{V(meso)}{\frac{4}{3}\pi(\frac{D}{2})^3}}$, n is molecule number in each nanocage, N is molar of Rh in per gram of solid catalyst, Vmeso is pore volume of FDU-12 or C-FDU-12, D is pore diameter of FDU-12 or C- FDU-12. [f] the Rh content quantified by ICP is 0.124 mmol/g which is similar with the result gained by UV-Vis.

In previous studies, the ratio of Rh/MonoPhos was varied from 1 to 3 for the asymmetric hydrogenation of olefins. It has been proven that the MonoPhos/Rh ratio significantly influenced the catalytic activity. Feringa has demonstrated the co-existence of

5   different rhodium species coordinated with 1, 2, or 3 ligands and 1 substrate molecule during the hydrogenation of methyl 2-acetamidocinnnamate at MonoPhos/Rh ratio of 2 using electrospray mass spectrometry. A positive non-linear effect was also discovered, which confirms the presence of Rh-complexes

10   with more than one ligand.[9e] It has been reported that higher ligated rhodium species such as RhL$_3$ or RhL$_4$ is inactive, but there is still insufficient evidence to conclude if the active catalytic species carries one or two ligands. In order to investigate the catalytic performance of solid catalysts with different

15   MonoPhos/Rh ratios and the possible influence of confined space on the transformation of different Rhodium species, Rh(MonoPhos)$_1$ and Rh(MonoPhos)$_3$ were also encapsulated in the nanocages of FDU-12.

Textural properties of Rh(MonoPhos)$_n$@FDU-12 and

20   Rh(MonoPhos)$_2$@C-FDU-12 are detected by the N$_2$ sorption experiment, and the results are summarized in Fig. 2 and Table 1. FDU-12 and C-FDU-12 exhibit high surface area, large pore size and pore volume, which is beneficial for the accommodation of molecular catalysts. The N$_2$ sorption isotherms are of type IV

25   pattern, showing that all samples possess mesoporous structure. It should be mentioned that the amount of micropore decreases quite a lot after encapsulation. Compared with parent FDU-12 or C-FDU-12, the BET surface area and pore volume of solid catalysts decrease significantly. For example, the BET surface

30   area and pore volume of Rh(MonoPhos)$_2$@C-FDU-12 decreased from 746 to 244 m^2/g and 0.64 to 0.20 cm^3/g respectively. For Rh(MonoPhos)$_2$@FDU-12, the BET surface area and total pore volume decreases respectively from 360 to 45 m^2/g and 0.41 to 0.057 cm^3/g as the Rh content increases from 0.03 to 0.16

35   mmol/g. The decrease in the BET surface area and total pore

volume is mainly due to the occupation of Rh-MonoPhos in the nanocages and the decrease in the amount of micropore of FDU-12 or C-FDU-12 after encapsulation.
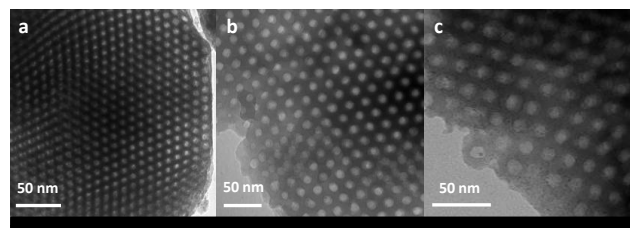
40   **Fig.3** TEM images of (a) FDU-12, (b) Rh(MonoPhos)$_2$@FDU-12 (0.12 mmol Rh /g), and (c) Rh(MonoPhos)$_2$@FDU-12 treated at 300 °C under air and then at 400 °C under H$_2$.
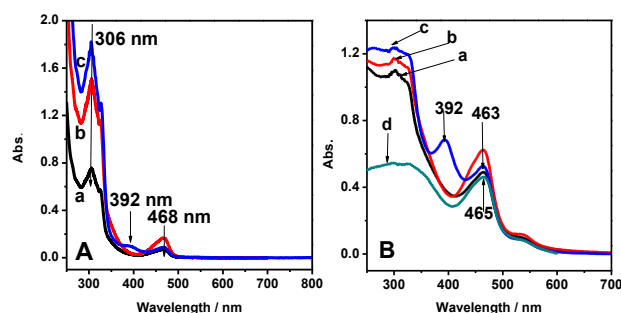
Fig.4 (A) UV-Vis spectra of (a) Rh(MonoPhos)$_1$, (b) Rh(MonoPhos)$_2$ and
45   (c) Rh(MonoPhos)$_3$ in dichloromethane and (B) the diffusion reflectance spectra of (a) Rh(MonoPhos)$_1$@FDU-12, (b) Rh(MonoPhos)$_2$@FDU-12, (c) Rh(MonoPhos)$_3$@FDU-12, and (d) Rh(MonoPhos)$_2$@C-FDU-12.

Transmission electron microscopy (TEM) images of FDU-12 and Rh(MonoPhos)$_2$@FDU-12 are shown in Fig. 3. Apparently,
50   both FDU-12 and Rh(MonoPhos)$_2$@FDU-12 (0.12 mmol Rh /g) have similar cubic Im3m structure, showing that the mesoporous

structure is retained after the encapsulation of Rh-MonoPhos. In order to investigate the dispersing degree of Rh-MonoPhos on silica supports, Rh(MonoPhos)$_2$@FDU-12 was treated at 300 ^{o}C under air and then at 400 ^{o}C under H$_2$. Through these treatments,
[5] metal complexes are converted to Rh nanoparticles. The TEM image shows that Rh nanoparticles with particle size of 1-3 nm are mainly dispersed in the nanocages of FDU-12, suggesting that

dichloromethane as solvent (Fig. 5). The main ion peaks at m/z = 194.9, 553.7, 820.7, 912.8, 1179.7 and 1539.5 are assigned to rhodium species of Rh(nbd), Rh(nbd)L, RhL$_2$, RhL$_2$(nbd), RhL$_3$
[35] and RhL$_4$ (L = MonoPhos), respectively. The ion peak at 375.9 present in the spectrum of MonoPhos/Rh = 3 might be assigned to the ligand and that at 194.9 is from the metal precursor. In the solution of MonoPhos/Rh = 1, Rh(nbd)L and RhL$_2$(nbd) could be
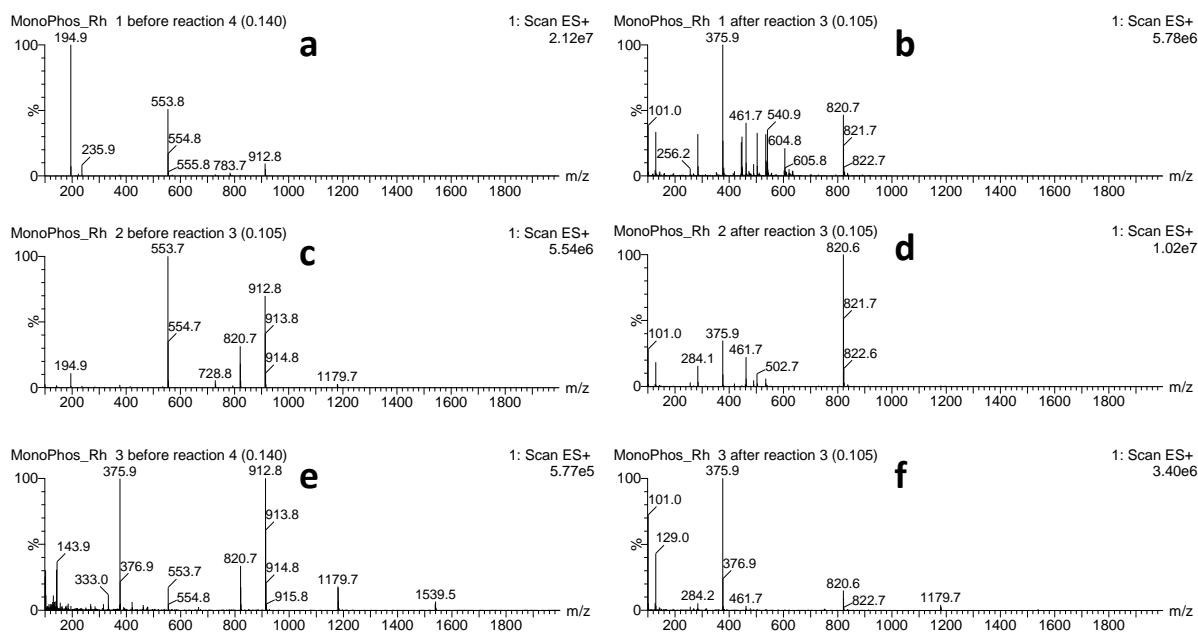
Fig.5 ESI-MS spectra of Rh-MonoPhos complexes in dichloromethane solution before (**a**, **c**, **e**) and after (**b**, **d**, **f**) the hydration reaction of itaconic acid dimethyl ester. **a**, **b**: MonoPhos/Rh = 1; **c**, **d**: MonoPhos/Rh = 2; **e**, **f**: MonoPhos/Rh = 3.

Rh-MonoPhos are distributed uniformly in the nanocages of FDU-12.
[10] The UV-Vis spectra of Rh-MonoPhos in dichloromethane and diffusion reflectance spectra of solid catalysts with different MonoPhos/Rh ratios are shown in Fig. 4. All the homogeneous catalysts with the MonoPhos/Rh ratio of 1, 2, or 3 show two main bands at λ_{max} = 306 nm (π-π* transition of naphthyl ring on
[15] MonoPhos ligand), λ_{max} = 468 nm (d-d transition of metal Rh). The UV-Vis spectrum of Rh(MonoPhos)$_3$ displays an extra band at λ_{max} = 392 nm. This is probably due to the existence of different Rh-MonoPhos species at high MonoPhos/Rh ratio. The solid catalysts show similar absorbance bands with their
[20] corresponding homogeneous catalysts with the exception that blue shift of the bands could be observed, suggesting a weak host-guest interaction between the nanocages and Rh-MonoPhos complexes. Notably, Rh(MonoPhos)$_2$@C-FDU-12 exhibits smaller blue shift than Rh(MonoPhos)$_2$@FDU-12(465 nm vs 463
[25] nm), suggesting that the inner surface carbon could decrease the interaction strength between molecular catalysts and the nanocages.
    To investigate the rhodium species of Rh-MonoPhos in solution and the possible transformation between different
[30] species during the hydrogenation process, ESI-MS was employed to characterize Rh-MonoPhos before and after reaction using

observed with Rh(nbd)L as dominant species. After
[40] hydrogenation reaction, Rh(nbd)L disappears and RhL$_2$ appears. Which MonoPhos/Rh = 2, the Rh(nbd)L, RhL$_2$, RhL$_2$(nbd) and RhL$_3$ co-exist in the solution with Rh(nbd)L and RhL$_2$(nbd) as dominant species. After reaction the ion signal of RhL$_2$ becomes dominant and that for Rh(nbd)L cannot be clearly observed.
[45] Increasing MonoPhos/Rh ratio to 3, the ion peaks for Rh(nbd)L, RhL$_2$, RhL$_2$(nbd), RhL$_3$ and RhL$_4$ could all be clearly observed with ligand and RhL$_2$(nbd) as dominant species. After reaction, signal for RhL$_3$ could be observed in addition to that of RhL$_2$, however, the ligand still remains as the dominant specie. The
[50] ESI-MS results suggest that different rhodium species definitely exist in the solution and high ratio of MonoPhos/Rh results in the formation of more complicated metal complexes, which is consistent with the literature reports.[9e] The comparison results before and after reaction also indicated that the transformation of
[55] metal complexes occurs indeed during the catalytic process.
    The catalytic performance of homogeneous and solid catalysts is tested in the asymmetric hydrogenation of itaconic acid dimethyl ester, which is one of the most commonly used substrates in the asymmetric hydrogenation reactions (Table 2).
[60] For homogeneous catalysts, Rh-MonoPhos complexes with MonoPhos/Rh ratio of 1, 2, and 3 are all active and enantioselective for the reaction. The TOF decreases in the order

of Rh(MonoPhos)$_2$ > Rh(MonoPhos)$_1$ > Rh(MonoPhos)$_3$. Rh(MonoPhos)$_2$ affords the highest activity and enantioselectivity, while Rh(MonoPhos)$_1$ shows the lowest enantioselectivity, which is different from the literature reports that Rh(MonoPhos)$_1$
[5] exhibits similar activity and enantioselectivity to Rh(MonoPhos)$_2$. The difference is probably due to the different reaction conditions employed in this work and

Table 2. The catalytic performance of solid catalysts with different MonoPhos/Rh ratios and different contents of Rh(MonoPhos)$_2$ in the
[10] nanocages for the asymmetric hydrogenation of itaconic acid dimethyl ester [a]

catalyst
10 bar H$_2$, 25 °C

Catalyst	Rh content (mmol/g)	Conv. (%)[b]	Ee. (%)[b]	TOF (/h)[c]
Rh(MonoPhos)$_1$@FDU-12	0.12	53(>99)	88(90)	1080(2580)
Rh(MonoPhos)$_2$@FDU-12	0.12	98(>99)	92(91)	1812(2712)
Rh(MonoPhos)$_3$@FDU-12	0.10	96(>99)	93(91)	1560(2136)
Rh(MonoPhos)$_2$@FDU-12	0.03	91	92	1356
Rh(MonoPhos)$_2$@FDU-12	0.07	99	93	1776
Rh(MonoPhos)$_2$@FDU-12	0.16	92	92	1608
Rh(MonoPhos)$_2$@C-FDU-12	0.13	>99	93	2052

[a] Reaction conditions: S/C=1000, 10 bar H$_2$, 3 mL dichloromethane, 2.5 mmol substrate, 25 °C, reaction time 90 min. The reaction condition was the same as heterogeneous one except that molecular catalysts were used. [b] Analysis by GC. [c] Turn over frequency. The TOF was defined as mmol substrate converted per Rh per hour with conversion obtained in initial 5 min (the kinetic plots of all the catalysts are performed and conversion in 5 min is less than 30 %). The values in the parentheses are for homogeneous catalysts.

in the literature. This also suggests that the catalytic system is very sensitive to the reaction conditions. The combined results of
[15] ESI-MS and catalysis suggest that RhL$_2$(nbd) may be the active species or the precursors for the active species.

Rh(MonoPhos)$_n$@FDU-12 (n=1, 2, 3) with Rh(MonoPhos)$_n$ encapsulated in the nanocages of FDU-12 could also catalyze the reaction with high activity and enantioselecitivity. The TOF of
[20] Rh(MonoPhos)$_n$@FDU-12 decrease in the order of Rh(MonoPhos)$_2$@FDU-12 > Rh(MonoPhos)$_3$@FDU-12 > Rh(MonoPhos)$_1$@FDU-12. Rh(MonoPhos)$_2$@FDU-12 showed the highest activity though its BET surface area is lower than other catalyst (Table 1). Compared with homogeneous
[25] counterparts, Rh(MonoPhos)$_n$@FDU-12 (n=1, 2, 3) displays lower activity, probably due to the limitation of mass transfer for the solid catalysts. Rh(MonoPhos)$_2$@FDU-12 and Rh(MonoPhos)$_3$@FDU-12 could retain 67~73% activity of their homogeneous counterparts (The ratios of retained activity are
[30] obtained by the comparison of TOF values of solid catalysts with their corresponding homogeneous catalysts. For example, the TOF of solid catalyst Rh(MonoPhos)$_2$@FDU-12 is 1812, its corresponding homogeneous catalyst is 2712, the retained ratio of activity is 1812/2712=67%). However, Rh(MonoPhos)$_1$@FDU-

[35] 12 only exhibited ~ 42% activity of the homogeneous one. The ESI-MS results in Fig. 5 show that only small amount of Rh(nbd)L$_2$ could be detected before the reaction for Rh(MonoPhos)$_1$ and more amount of Rh(nbd)L$_2$ and RhL$_2$ were formed after the reaction. Thus it is reasonable to suspect that the
[40] much lower activity of Rh(MonoPhos)$_1$@FDU-12 might suggest that the formation of RhL$_2$ species is not as free in the nanocages as in solution. As a result, smaller amounts of active species could be formed in nanocages during the catalytic process. The limited transformation of different species in nanocages benefits
[45] the mechanism investigation especially for metal complexes with the co-existence of various species. The enantioselectivity of Rh(MonoPhos)$_n$@FDU-12 (n=2, 3) is slightly higher than the homogeneous counterparts, probably due to positive effect of the confined nanospace.

[50] The catalytic performance of Rh(MonoPhos)$_2$@FDU-12 with different metal complex loading is also investigated (Table 2). Increasing the Rh content from 0.03~0.16 mmol/g, the activity (TOF) of solid catalyst increases firstly, and reaches the maximum with content of 0.12 mmol/g (TOF 1812 h^{-1}). After that,
[55] the activity of the solid catalyst decreases by further increasing the Rh loading. The "volume active site density" of the nanocages can be used to explain this tendency. With the increase in Rh loading from 0.03 to 0.12 mmol/g, the number of catalyst molecule in each cage increases from 63 to 237 (Table 1).
[60] Consequently, the contact frequency between substrates and catalysts becomes increased and the activity of the solid catalyst also increased. At high catalyst loading, the nanocage becomes crowded, and the corresponding surface area and pore volume are low, which makes the diffusion of reactants and products in the
[65] nanocage difficult during the catalytic process, which results in the decrease in the activity of the solid catalyst.
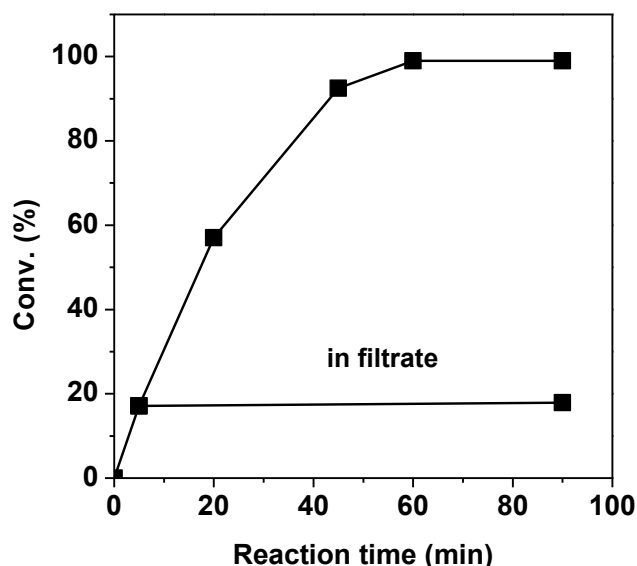
Fig.6 Kinetic plots of asymmetric hydrogenation of itaconic acid dimethyl ester on the solid catalyst Rh(MonoPhos)$_2$@C-FDU-12 (0.13
[70] mmol Rh /g) and in the filtration experiment.

It has been demonstrated that the microenvironment can influence the interaction of the molecular catalysts with the

supports and the diffusion of reactants and products in the nanocages significantly.[7, 17] For modifying the microenvironment of the nanocages, C-FDU-12 which is synthesized by carbonization of as-made FDU-12 at 500 °C in N_2 instead of air
[5] (5 wt% carbon) was used as host materials. Rh(MonoPhos)$_2$@C-FDU-12 showed higher activity than Rh(MonoPhos)$_2$@FDU-12 under similar reaction conditions with TOF up to 2052 h^{-1}. Considering the fact that C-FDU-12 has different H_2O/benzene adsorption ratio with FDU-12 (2.96 versus 4.58), the improved
[10] diffusion rate of hydrophobic reactants should be one of the reasons for the improved activity. Based on the results of N_2 sorption and the UV-Vis diffusion reflectance spectra, Rh(MonoPhos)$_2$@C-FDU-12 has higher BET surface area and pore volume but weaker interaction of Rh(MonoPhos)$_2$ with the
[15] nanocages than Rh(MonoPhos)$_2$@FDU-12. Thus the higher catalytic performance of Rh(MonoPhos)$_2$@C-FDU-12 might also be attributed to its higher BET surface area and the inner carbonized surface that could decrease the interaction between molecular complex and support, which is beneficial for keeping
[20] the intrinsic properties of the molecular catalyst.

Table 3. Asymmetric hydrogenation of olefin derivatives (**a** - **d**) on Rh(MonoPhos)$_2$@FDU-12 and Rh(MonoPhos)$_2$@C-FDU-12.[a]

RO_2C —— CO_2R R' —— CO_2Me / NHAc
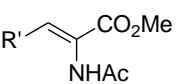
R = Me (**a**)   R' = H (**c**)
R = H (**b**)   R' = Me (**d**)

Catalyst	Substrate	S/C	Reaction time (h)	Conv. (%)	Ee. (%)
Rh(MonoPhos)$_2$@ FDU-12	**a**	500	0.75	>99	93
	a	1000	1.5	98	92
	a	2000	4	86	92
Rh(MonoPhos)$_2$@ C-FDU-12	**a**	2000	4	>99	92
	a	1000	1	>99	92
Rh(MonoPhos)$_2$@ FDU-12[b]	**b**	200	1	89	89
Rh(MonoPhos)$_2$@ C-FDU-12[b]	**b**	200	1	>99	89
Rh(MonoPhos)$_2$@ FDU-12	**c**	1000	12	65	96
Rh(MonoPhos)$_2$@ C-FDU-12	**c**	1000	12	>99	96
Rh(MonoPhos)$_2$@ FDU-12	**d**	1000	12	26	96
Rh(MonoPhos)$_2$@ C-FDU-12	**d**	1000	12	96	96

[a] Reaction conditions: 10 bar H_2, 3 mL dichloromethane, 2.5 umol Rhodium, 25 °C. [b] [S]=0.04 M. Rh(MonoPhos)$_2$@FDU-12 (0.12 mmol Rh /g), Rh(MonoPhos)$_2$@C-FDU-12 (0.13 mmol Rh /g). The conversion and ee values are analyzed by GC.

For further investigating the catalytic performance of
[25] Rh(MonoPhos)$_2$@C-FDU-12, the catalytic kinetic plots were recorded (Fig. 6). As the reaction time increases, the conversion of itaconic acid dimethyl ester rapidly increases. To exclude the conversion contribution from the leached Rh species in the solution, the reaction is stopped after 17.1% consumption of the
[30] reactant and the filtrate is immediately isolated through a rapid centrifugation. The filtrate is continuously stirred under the same

reaction condition, but almost no increasing of the conversion could be found. These results confirm that the catalytic activity is truly contributed by Rh(MonoPhos)$_2$ confined in the nanocages.
[35] Encouraged by the superior performance of the solid catalyst in asymmetric hydrogenation of itaconic acid dimethyl ester, other olefin derivatives have been employed (Table 3). All the substrates can be smoothly transformed into desirable products with good to excellent enantioselectivity, however, the reaction
[40] rates for different substrates vary considerably. For example, substrate **a** can almost be converted completely on Rh(MonoPhos)$_2$@FDU-12 at S/C = 1000 in 1.5 h, but substrates **c** and **d** only get 65% and 26% conversion even in 12 h, respectively. Rh(MonoPhos)$_2$@C-FDU-12 exhibits significantly
[45] higher activity than Rh(MonoPhos)$_2$@FDU-12, especially for **c** and **d**. For example, Rh(MonoPhos)$_2$@C-FDU-12 could afford 96% conversion for substrate **d** at S/C = 1000 in 12 h, while the conversion is only 26% for Rh(MonoPhos)$_2$@FDU-12 under the same reaction conditions. Rh(MonoPhos)$_2$@C-FDU-12 and
[50] Rh(MonoPhos)$_2$@FDU-12 have similar enantioselectivity. The higher activity of Rh(MonoPhos)$_2$@C-FDU-12 is due to the combined results of its high surface hydrophobicity and high BET surface area and weak interaction of Rh(MonoPhos)$_2$ with nanocages as we discussed above.
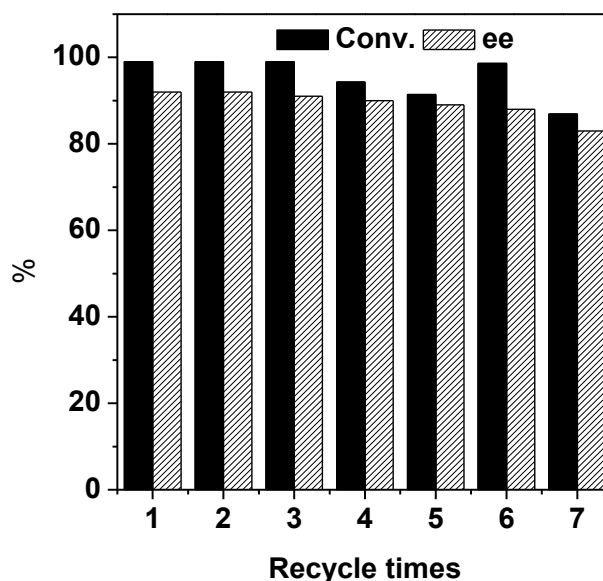
[55]
Fig.7 Recyclability of Rh(MonoPhos)$_2$@C-FDU-12 (0.13 mmol Rh /g) in the asymmetric hydrogenation of itaconic acid dimethyl ester (the reaction time is 45 min, 60 min, 95 min, 2h, 3 h, 5 h, and 7 h for cycle 1, 2, 3, 4, 5, 6 and 7, respectively).

[60] The recyclability of the solid catalyst was tested by using Rh(MonoPhos)$_2$@-FDU-12 as a model catalyst in the asymmetric hydrogenation of itaconic acid dimethyl ester (Fig. 7). As can be seen, the solid catalyst can be reused more than 7 times with little loss of the activity and enantioselectivity. Toward the end of
[65] recycle, longer reaction time is needed to obtain high conversion, and the enantioselectivity decreases a little. This is probably due to the dissociation of metal and ligands during the recycle process. On the other hand, the broken of the solid catalyst structure may be another influential factor on the deactivation of the solid

catalyst. After recycling, the BET surface area and total pore volume decreased from 244 to 8 m^2/g and 0.20 to 0.025 cm^3/g respectively.

Conclusions

In summary, we have demonstrated the successful encapsulation of asymmetric multicomponent catalyst, Rh-MonoPhos, in the nanocages of mesoporous silicas using TMOS as silylation reagent. The solid catalyst shows excellent catalytic performance (TOF 2052 h^{-1}, 93% ee) in asymmetric hydrogenation reaction of itaconic acid derivatives and N-acetydehydroamino acids derivatives. The TOF of Rh(MonoPhos)$_n$@FDU-12 decrease in the order of Rh(MonoPhos)$_2$@FDU-12 > Rh(MonoPhos)$_3$@FDU-12 > Rh(MonoPhos)$_1$@FDU-12. In combination with ESI-MS result, the active species for the reaction should involve Rh(MonoPhos)$_2$. Moreover, through tuning the microenvironment of FDU-12 by coating a thin layer of carbon onto the inner surface, the catalytic activity of solid catalyst can be further improved. This work provides a new strategy to realize the heterogenization of the multicomponent catalyst Rh-MonoPhos, which might also be applicable in other catalytic systems.

Experimental

Chemicals and materials

Pluronic F127 (EO$_{106}$PO$_{70}$EO$_{106}$) and itaconic acid dimethyl ester were purchased from Sigma Aldrich. Tetramethylorthosilicate (TMOS, AR) and tetraethylorthosilicate (TEOS, AR) were purchased from Shanghai Chemical Reagent Company of the Chinese Medicine Group. Anhydrous dichloromethane and hexane were purchased from Beijing InnoChem Science and Technology Company. Metal precursor, bis(norbornadiene)rhodium(I) tetrafluoroborate, was purchased from Alfa Aesar. The ligand, monodentate phosphoramidite (MonoPhos), was synthesized according to the literature method.[35] FDU-12 was synthesized according to the reported method.[36] C-FDU-12 was synthesized by carbonization of as-made FDU-12 in N_2 at 500 ^{o}C instead of air.

The procedure for the preparation of solid catalysts

Rh(MonoPhos)$_2$@FDU-12: All the manipulations were performed under argon atmosphere using standard Schlenk techniques. FDU-12 (0.5 g) which was already vacuumed at room temperature for 6 h was dispersed in anhydrous CH_2Cl_2 (2 mL) containing Rh-MonoPhos (0.025, 0.05, 0.075 or 0.10 mmol) with MonoPhos/Rh ratio of 2 at room temperature. After stirring for 4 h, CH_2Cl_2 was removed by evaporation. Subsequently, a solution of prehydrolyzed TMOS, prepared by stirring 6 mmol of deoxidized TMOS and 54 mg of deoxidized H_2O for 2.5 h at room temperature, was added to the above mixture, followed by the addition of deoxidized hexane (1.0 mL). After stirring at room temperature for 8 h, the resultant solid was isolated by centrifugation and washed with anhydrous CH_2Cl_2 for several times to remove Rh-MonoPhos adsorbed on the outside surface of FDU-12. The solid product was dried under vacuum and the Rh contents were quantified by UV-Vis.

Rh(MonoPhos)$_2$@C-FDU-12 was prepared in a similar method to Rh(MonoPhos)$_2$@FDU-12 with the exception that C-FDU-12 was used as solid support.

Rh(MonoPhos)$_1$@FDU-12 and Rh(MonoPhos)$_3$@FDU-12 were prepared in a similar method to Rh(MonoPhos)$_2$@FDU-12 using 0.075 mmol of Rh-MonoPhos with MonoPhos/Rh ratio of 1 and 3, respectively.

Characterization

Nitrogen physical adsorption measurement was carried out on micrometritics ASAP2020 volumetric adsorption analyzer. Before the measurements, the samples were degassed at 393 K for 5 h. The BET surface area was evaluated from the data in the relative pressure range P/P_0 of 0.05 to 0.25. The total pore volume was estimated from the amount adsorbed at the P/P_0 value of 0.99. The pore diameter was determined from the adsorption branch by the BJH method. UV-Vis spectra were recorded on a SHIMADZU UV-Vis 2550 spectrophotometer. Diffuse-reflectance UV-Vis spectra were also recorded on the SHIMADZU UV-Vis 2550 spectrophotometer using $BaSO_4$ as the reference. XRD patterns were recorded on a Rigaku RINT D/Max-2500 powder diffraction system by using $Cu_{K\alpha}$ radiation. Transmission electron microscopy (TEM) was performed using a FEI Tecnai G2 Spirit at an acceleration voltage of 120 kV. ESI-MS experiments were performed on a ZQ single quadrupole mass spectrometer from Waters Corporation.

General procedure for the asymmetric hydrogenation reactions

Anhydrous dichloromethane (3 mL) and itaconic acid dimethyl ester (2.5 mmol, 395 mg) were added to a test tube containing desired amount of Rh(MonoPhos)$_n$@FDU-12 or Rh(MonoPhos)$_2$@C-FDU-12 (2.5 umol Rh) under nitrogen atmosphere. The test tube was transferred into a stainless steel autoclave and sealed. After purging with H_2 for several times, the pressure was adjusted to 10 bar and left to stir at 25 ^{o}C in a constant temperature bath. After reaction, H_2 pressure was released and the solid chiral catalyst was separated with centrifugation. The conversion and enantiomeric excess were analyzed by chiral gas chromatography using a Supelco γ-DEX 225 capillary column (30 m × 0.25 mm × 0.25 mm). For recycling test, the solid catalyst obtained by centrifugation in glovebox under nitrogen was used directly for the next catalytic cycle.

Acknowledgements

Notes and references

[a] State Key Laboratory of Catalysis, Dalian Institute of Chemical Physics, Chinese Academy of Sciences, 457 Zhongshan Road, Dalian 116023, China
[b] University of Chinese Academy of Sciences, Beijing 100049, China
[c] These authors contributed equally to this research.
* To whom correspondence should be addressed. E-mail: yangqh@dicp.ac.cn; Fax: 86-411-84694447. URL: http://www.hmm.dicp.ac.cn ; canli@dicp.ac.cn

1. (a) Noyori, R., Angew. Chem., Int. Ed., 2002, 41, 2008-2022; (b) Chelucci, G., Coord. Chem. Rev., 2013, 257, 1887-1932; (c) Aikawa, K.; Mikami, K., J. Synth. Org. Chem. Jpn., 2012, 70, 1281-1294; (d) Broere, D. L. J.; Ruijter, E., Synthesis, 2012, 44, 2639-2672; (e) Cadu, A.; Andersson, P. G., J. Organomet. Chem., 2012, 714, 1-9; (f) Rueping, M.; Bootwicha, T.; Kambutong, S.; Sugiono, E., Chem. Asian J., 2012, 7, 1195-1198; (g) Wang, F. J.; Liu, L. J.; Wang, W. F.; Li, S. K.; Shi, M., Coord. Chem. Rev., 2012, 256, 804-853; (h) Bauer, E. B., Synthesis, 2012, 44, 1131-1151; (i) Royo, B.; Peris, E., Eur. J. Inorg. Chem., 2012, 1309-1318.

2. Carreiro, E. P.; Moura, N. M. M.; Burke, A. J., Eur. J. Org. Chem., 2012, 518-528.

3. Fraile, J. M.; Garcia, J. I.; Mayoral, J. A., Chem. Rev., 2009, 109, 360-417.

4. De Decker, J.; Bogaerts, T.; Muylaert, I.; Delahaye, S.; Lynen, F.; Van Speybroeck, V.; Verberckmoes, A.; Van der Voort, P., Mater. Chem. Phys., 2013, 141, 967-972.

5. (a) Wan, Y.; McMorn, P.; Hancock, F. E.; Hutchings, G. J., Catal. Lett., 2003, 91, 145-148; (b) Baleizao, C.; Gigante, B.; Garcia, H.; Corma, A., J. Catal., 2003, 215, 199-207.

6. (a) Jones, M. D.; Raja, R.; Thomas, J. M.; Johnson, B. F.; Lewis, D. W.; Rouzaud, J.; Harris, K. D., Angew. Chem. Int. Ed., 2003, 42, 4326-31; (b) Liu, X.; Wang, P. Y.; Zhang, L.; Yang, J.; Li, C.; Yang, Q. H., Chem. Eur. J., 2010, 16, 12727-12735; (c) Zhang, L.; Liu, J.; Yang, J.; Yang, Q. H.; Li, C., Chem. Asian J., 2008, 3, 1842-1849.

7. Bai, S. Y.; Yang, H. Q.; Wang, P.; Gao, J. S.; Li, B.; Yang, Q. H.; Li, C., Chem. Commun., 2010, 46, 8145-7.

8. Wang, D. S.; Chen, Q. A.; Lu, S. M.; Zhou, Y. G., Chem. Rev., 2012, 112, 2557-2590.

9. (a) Alegre, S.; Alberico, E.; Pamies, O.; Dieguez, M., Tetrahedron: Asymmetry, 2014, 25, 258-262; (b) Frank, D. J.; Franzke, A.; Pfaltz, A., Chem. Eur. J., 2013, 19, 2405-2415; (c) Duan, Z. C.; Wang, L. Z.; Hu, X. P.; Zheng, Z., J. Mol. Catal. (China), 2012, 26, 328-332; (d) Minnaard, A. J.; Feringa, B. L.; Lefort, L.; De Vries, J. G., Acc. Chem. Res., 2007, 40, 1267-1277; (e) van den Berg, M.; Minnaard, A. J.; Haak, R. M.; Leeman, M.; Schudde, E. P.; Meetsma, A.; Feringa, B. L.; de Vries, A. H. M.; Maljaars, C. E. P.; Willans, C. E.; Hyett, D.; Boogers, J. A. F.; Henderickx, H. J. W.; de Vries, J. G., Adv. Synth. Catal., 2003, 345, 308-323; (f) Jerphagnon, T.; Renaud, J. L.; Bruneau, C., Tetrahedron: Asymmetry, 2004, 15, 2101-2111; (g) Pena, D.; Minnaard, A. J.; de Vries, A. H. M.; de Vries, J. G.; Feringa, B. L., Org. Lett., 2003, 5, 475-478.

10. (a) Chen, W. P.; Roberts, S. M.; Whittall, J., Tetrahedron Lett., 2006, 47, 4263-4266; (b) Simons, C.; Hanefeld, U.; Arends, I.; Maschmeyer, T.; Sheldon, R., J. Catal., 2006, 239, 212-219; (c) Shi, L.; Wang, X. F.; Sandoval, C. A.; Wang, Z.; Li, H. J.; Wu, J.; Yu, L.T.; Ding, K. L, Chem. Eur. J., 2009, 15, 9855-67.

11. Wang, X. W.; Ding, K. L., J. Am. Chem. Soc., 2004, 126, 10524-5.

12. Simons, C.; Hanefeld, U.; Arends, I.; Sheldon, R. A.; Maschmeyer, T., Chem. Eur. J., 2004, 10, 5829-5835.

13. Zhang, X. M.; Liu, X.; Peng, J.; Zhao, Y. P.; Yang, Q. H., Catal. Sci. Technol., 2014, 4, 1012-1016.

14. Liu, X.; Bai, S. Y.; Yang, Y.; Li, B.; Xiao, B.; Li, C.; Yang, Q. H., Chem. Commun., 2012, 48, 3191-3.

15. van den Berg, M.; Minnaard, A. J.; Schudde, E. P.; van Esch, J.; de Vries, A. H. M.; de Vries, J. G.; Feringa, B. L., J. Am. Chem. Soc., 2000, 122, 11539-11540.

16. Fan, J.; Yu, C. Z.; Lei, J.; Zhang, Q.; Li, T. C.; Tu, B.; Zhou, W. Z.; Zhao, D. Y., J. Am. Chem. Soc., 2005, 127, 10794-10795.

17. Li, B.; Bai, S. Y.; Wang, P.; Yang, H. Q.; Yang, Q. H.; Li, C., Phys. Chem. Chem. Phys., 2011, 13, 2504-11.

Colour graphic	R=Me, H; R'=H, Me ● Rh-MonoPhos$_x$
Highlight	Encapsulated multicomponent catalyst, Rh-MonoPhos, in nanoreactors showed excellent catalytic activity in the asymmetric hydrogenation reactions.